3.3. Cytotoxicity

The cytotoxicities of CL and CL/Brij 35/sito-G encapsulating asODN at the concentrations from 0 to 9 μM (asODN) were determined by MTT assay, respectively. As shown in Fig. 4, the cytotoxicities of both cationic liposomes were increased with the elevation of asODN concentration, particularly in the high concentration range from 3.6 to 9.0 μM. The increased cytotoxicity may be caused by the cationic lipid DC-Chol, since the DC-Chol concentration was elevated accompanied with the elevation of asODN concentration. However, there was no significant difference in the cell viability between CL and CL/Brij 35/sito-G group in the tested concentration range. This indicated that the co-modification of Brij 35 and sito-G brought little influence to the cytotoxicity of cationic liposomes.

3.4. Cellular uptake and intracellular distribution in fluorescence microscopy and CLSM

After treated with CL/Brij 35/sito-G encapsulating 1.8 μM of FITC-asODN, the cells were observed through the fluorescence microscopy. Consistent with the results of transfection efficiency (Fig. 1) and antigens production (Fig. 2), most cells showed strong fluorescence intensity (data not shown), indicating that CL/Brij 35/sito-G led to high transfection efficiency. Besides, it could be observed that the cell-associated fluorescence intensity increased within the time period during 0 to 6 h and the fluorescence intensity at 24 h was similar to that at 6 h (data not shown).

In CLSM, FITC-asODN and rhodamine-DOPE for liposomes were used at the same time to serve as the fluorescence probes. In the CLSM images, the green, red and blue fluorescence indicated FITC-asODN, lipids and the nuclear, respectively. A series of CLSM section images (labelled as 1, 2,... and 8 from top to bottom of the cell in order) were obtained by scanning the primary rat hepatocytes at an interval of 1 μm thickness (Fig. 5). As shown in Fig. 5B, there was continuous green fluorescence in the nuclear which meant that the most amount of the asODN was distributed or accumulated in the nuclear lumen. The continuous red fluorescence appeared in the cytoplasm but not in the nuclear (Fig. 5C), and this might indicate the lipids or liposomes did not enter the nuclear lumen after penetrating into the cell. In the cytoplasm, especially near the nuclear, the punctuate green and red fluorescence appeared at the same place (Fig. 5D). In section B4–B6, a few punctuate fluorescence particles appeared on the cell membrane just like those in the cytoplasm, indicating some of the asODN-encapsulating liposomes was endocytosed to form endosomes. These fluorescence particles in the cytoplasm seemed to be the endosomes that had not yet released the asODN.

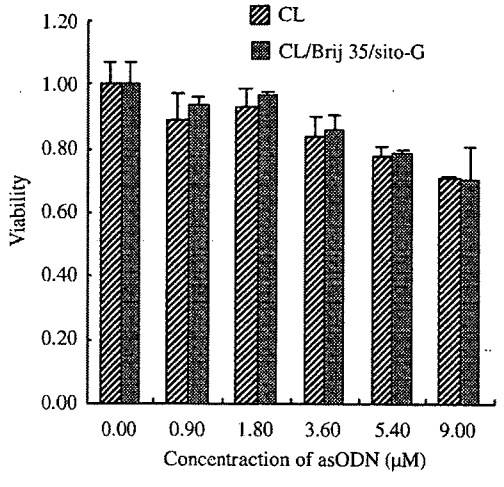

Fig. 4. Viability of HepG2.2.15 cells treated with CL and CL/Brij 35/sito-G at the concentrations from 0 to 9 μM of asODN for 3 days. The cell viability was determined by MTT assay. Each value represented the mean±S.D. (n=3).

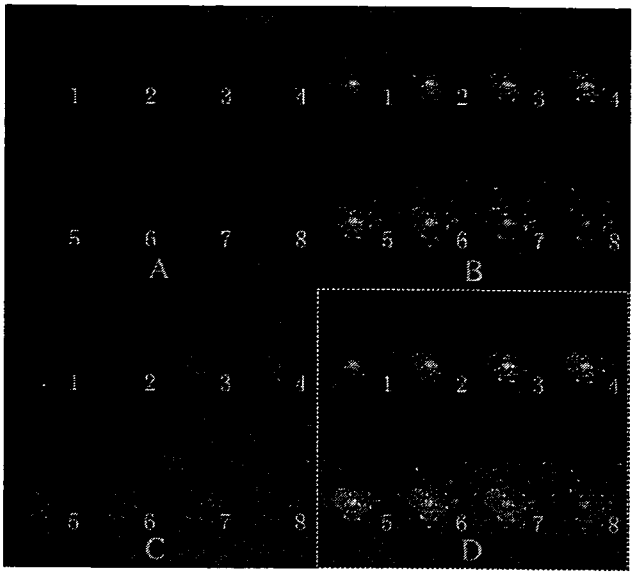

Fig. 5. Series of CLSM section images of the primary rat hepatocyte treated with CL/Brij 35/sito-G encapsulating FITC-asODN. The CL/Brij 35/sito-G was labelled with rhodamine by adding 1.0% (molar ratio) rhodamine-DOPE in the liposome formulation. The concentration of FITC-asODN was 1.8 μM. After treatment for 6 h, Hoechst 33258 was added into the medium to stain the nuclear for 30 min. The green, red, and blue fluorescence indicated FITC-asODN, the lipids, and the nuclear, respectively. The three groups of A, B and C were obtained from different excitation wavelengths. Group A showed the nuclear, group B showed the asODN, and group C showed the rhodamine labelled cationic liposomes. Group D was obtained by overlaying group A, B and C through the image process system of CLSM, and showed the overall fluorescence characteristics of the cell. (For interpretation of the references to colour in this figure legend, the reader is referred to the web version of this article.)

3.5. Mechanisms of the cellular uptake of CL/Brij 35/sito-G

The cellular uptake and delivery mechanisms of the encapsulated asODN in CL/Brij 35/sito-G were studied by evaluating the HBsAg inhibition effect of asODN in ELISA and by observing its intracellular distribution in CLSM.

In the presence of asialofetuin, the HBsAg inhibition effects of CL/sito-G and CL/Brij 35/sito-G were reduced, while that of

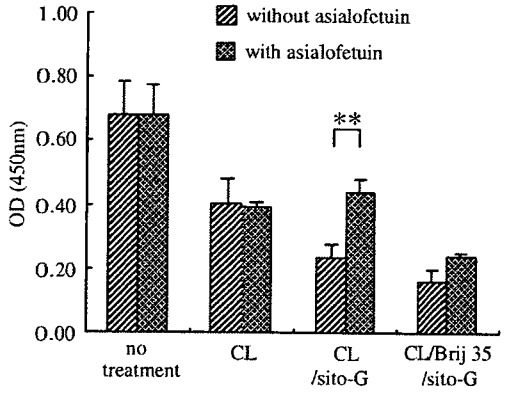

Fig. 6. Effect of asialofetuin on HBsAg inhibition effect of the asODN encapsulated in the cationic liposomes. HepG2.2.15 cells were treated with the cationic liposomes encapsulating asODN (3.6 μM) for 3 days, in the presence or absence of asialofetuin (1 mg/ml). The HBsAg production was determined by ELISA. Each value represented the mean±S.D.(n=3). **P<0.01, significantly different.

CL was not (Fig. 6). As the result, the inhibition effects of CL/sito-G and CL reached almost the same level. Asialofetuin decreased the HBsAg inhibition effects of the sito-G contained cationic liposomes (i.e. CL/sito-G and CL/Brij 35/sito-G) but affected little on the non-sito-G contained cationic liposomes (i.e. CL), because the recognition of ASGPR to sito-G could be blocked when the sito-G contained cationic liposomes were co-incubated with 1.0 mg/mL asialofetuin which could be recognized by ASGPR specifically. However there was no statistically significant difference between "with" and "without" asialofetuin for the HBsAg inhibition effect of CL/Brij 35/sito-G, in which Brij 35 seemed to decrease the specific recognition of ASGPR to sito-G in CL/Brij 35/sito-G. The phenomenon could be explained according to the followings: (1) Both Brij 35 and sito-G have amphiphilic structure and could insert into the bilayer membrane of liposomes. Since Brij 35 has a long PEG chain that could extend outside and bring steric hindrance [22], it might prevent part of ligands from binding with the surface receptor and thus decrease the specificity of CL/Brij 35/sito-G to hepatocytes; (2) Brij 35 compensated the transfection reduction induced by asialofetuin, because both sito-G and Brij 35 could enhance the transfection via different mechanisms, such as ASGPR pathway for sito-G and facilitating membrane fusion for Brij 35. Consequently when the effect of sito-G was blocked, the transfection reduction was not so much because of the transfection enhancement of Brij 35 through facilitating membrane fusion.

Wortmannin is known as an inhibitor of endocytosis [23]. When the cells were co-incubated with wortmannin, the antigens inhibition effect of CL/Brij 35/sito-G was drastically decreased by 70.7% for HBsAg (Fig. 7a) and 50.1% for HBeAg (Fig. 7b), compared with that of absence wortmannin group. This indicated that endocytosis was one of the uptake pathways for the encapsulated asODN.

Nigericin is known as an antibiotic that can dissipate the pH gradient across the endosome membrane and thus inhibit the delivery of asODN from the endosomes via membrane fusion [23]. When the cells were co-incubated with nigericin, the antigens inhibition effect of CL/Brij 35/sito-G was sharply decreased by 44.1% for HBsAg (Fig. 7a) and 46.2% for HBeAg (Fig. 7b). This suggested that nigericin inhibited the delivery of CL/Brij 35/sito-G from endosomes via membrane fusion between liposome and endosome membrane.

Fig. 8 showed us the CLSM images of the primary rat hepatocytes treated with CL/Brij 35/sito-G (Fig. 8a), and with CL/Brij 35/sito-G in the presence of wortmannin (Fig. 8b), nigericin (Fig. 8c) and asialofetuin (Fig. 8d), respectively. In the presence of wortmannin, there were lots of punctuate fluorescence particles (red and green) on the cell membrane but few or no in the cytoplasm, and only weak continuous fluorescence (red and green) in the cytoplasm and the nuclear. This showed us that wortmannin, an endocytosis inhibitor, inhibited the cellular uptake of CL/Brij 35/sito-G via endocytosis. In the presence of nigericin, there were more punctuate particles (red and green) in the cytoplasm than in the absence of nigericin, but very weak continuous fluorescence (red and green) in the cytoplasm and nuclear. A possible explanation was that after the liposomes entered the cells via endocytosis to form endosomes, nigericin inhibited the delivery of asODN from liposomes via membrane fusion between endosomes and liposomes. In the presence of asialofetuin, the cell showed similar fluorescence distribution but weaker fluorescence intensity compared with that in the absence of asialofetuin. This suggested that when the ASGPR-mediated endocytosis was blocked competitively by asialofetuin, the transmembrane ability of CL/Brij 35/sito-G was reduced, which was consistent with the previous results, i.e., the antisense effect of CL/Brij 35/sito-G in the absence of

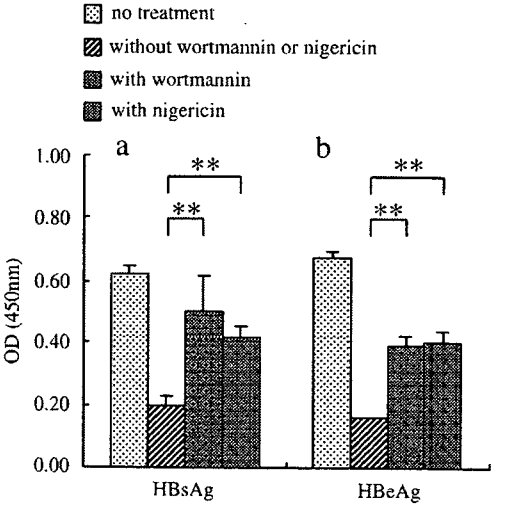

Fig. 7. Effect of wortmannin and nigericin on the antigens inhibition effect of the asODN encapsulated in CL/Brij 35/sito-G. HepG2.2.15 cells were treated with CL/Brij 35/sito-G encapsulating asODN (3.6 μM) for 3 days, in the presence or absence of wortmannin (0.1 μM) or nigericin (1.0 μM). The antigens production was determined by ELISA. Each value represented the mean±S.D. (n=3). **P<0.01, significantly different.

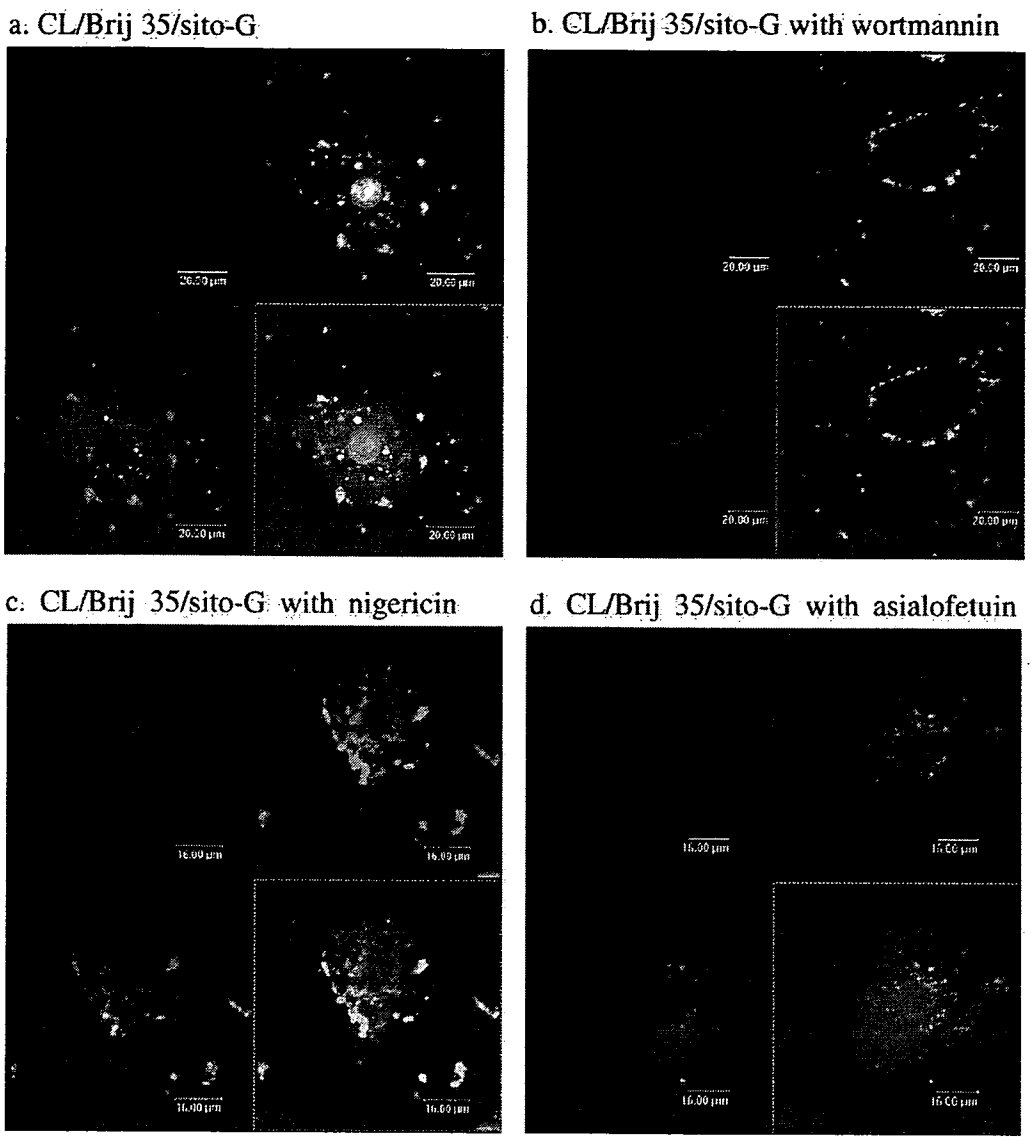

Fig. 8. CLSM images of the primary rat hepatocyte treated with CL/Brij 35/sito-G encapsulating FITC-asODN (1.8 μM). The CL/Brij 35/sito-G was labelled with rhodamine by adding 1.0% (molar ratio) rhodamine-DOPE in liposome formulations. The concentration of FITC-asODN was 1.8 μM. The inhibitors such as asialofetuin, wortmannin and nigericin were added into the medium with the final concentrations 1.0 g/ml, 0.1 μM and 1.0 μM, respectively. After treatment for 6 h, Hoechst 33258 was added into the medium to stain the nuclear. The green fluorescence indicated FITC-asODN, the red indicated the lipids and the blue indicated the nuclear. (For interpretation of the references to colour in this figure legend, the reader is referred to the web version of this article.)

asialofetuin was higher than that in the presence of asialofetuin (Fig. 6).

4. Discussion

In this study, the novel cationic liposomes co-modified with ligand and nonionic surfactant, was developed as a gene transfer carrier to deliver an anti-HBV asODN orientedly to the hepatocytes. Although the cellular uptake of asODN was dependant on cell types, cell culture conditions, media, sequences, length of the sequences etc., people usually took it for granted that gene (oligonucleotides and plasmids) could not enter the cells easily because of the strong electrostatic repulsion between the nucleotides chain and the cell membrane. Our results showed that free asODN could be taken up by hepatocytes even at the relatively low concentration (0.36 μM), despite insufficient antigens inhibition effect compared with the effect of the asODN encapsulated in cationic liposomes. The possible reason is the inherent strong uptake ability of hepatocytes, based on the large cell size and biological requirements for the strong metabolic ability of the liver. Similar to our results, Robaczewska et al. reported strong fluorescence intensity of the hepatocytes when injected with free FITC-asODN solution [24] and Soni et al. reported more efficient virus inhibition of free asODN solution than that of unmodified neutral asODN-encapsulating liposomes when injected to ducklings infected with duck HBV [25]. With the co-modification of Brij 35 and sito-G, CL/Brij 35/sito-G showed not only high efficient

transfection and antigens inhibition but hepatocyte-targeting effect based on the receptor binding competition test, and the co-modification did not increase cytotoxicity to the hepatocytes, even when the cells were treated with the cationic liposomes for as long as 3 days. Phosphorothioate oligonucleotides are known to be resistant to nuclease degradation, but not resistant to RNaseH degradation [26]. When the concentration of asODN in the cytoplasm was elevated to a certain level, there might be relatively more RNaseH to be activated quickly, and therefore the degradation of the asODN was accelerated. Besides, HepG2.2.15 is a cell line that can stably produce HBV mRNAs and antigens. In spite of the treatment with asODN, the HBV DNA integrated into the cell chromosome could still transcript more and more mRNAs all the time to make up for the degradation of the mRNA, so the virus or the virus antigens could not be cleared completely by the asODN, which was why the antigens inhibition was not complete.

Through CLSM, people could clearly observe the distribution of the fluorescence probes in the cells and get some detailed information about the intracellular behaviors of the liposomes and the asODN. It was known that when microinjected to the cytoplasm, free FITC-asODN could substantially accumulate in the nuclear rapidly by passive diffusion through the membrane. Interestingly, we found that asODN encapsulated in the co-modified cationic liposomes accumulate in the nuclear after transfer into the cells (Fig. 5). One of the possible reasons was that the asODN was recruited and immobilized by the interaction between asODN and the positively charged intra-nuclear components such as histones [27]. Another reason was that the asODN might be associated with the intracellular RNA matrix [28]. As for the antisense therapy, the accumulation of asODN in the nuclear was advantageous, because mRNA, which was aimed at by asODN, would be transcripted in the nuclear first and then diffuse out to the cytoplasm. In Figs. 5 and 8, there were many fluorescent particles near the nuclear or on the nuclear membrane, which suggested that maybe the endosomes were associated with the nuclear membrane and then the asODN would be delivered based on the membrane interaction. Shi et al. reported that the cationic liposomes–asODN complex was released from the artificially ruptured endosomes with the dissociation of cationic lipids and asODN at the nuclear membrane [28]. Some cationic polymers such as polyethylinemine (PEI) could mediate the entry of plasmid DNA into the nuclear at the nuclear membrane [29].

The ASGPR-mediated targeted gene carriers were developed by many groups, such as cationic liposomes, polymers, and recombinant lipoproteins, for the gene to be delivered to the liver, especially to hepatocytes. Since HBV only replicates in hepatocytes but does not in other cells, it is required to confirm the hepatocyte specificity of ligand in the liver-targeting gene delivery carrier. We already reported that the distribution of SG and Brij 35 co-modified liposomes in rat hepatocytes (containing ASGPR on the cell surface) were higher than in non-hepatocytes (containing no ASGPR), and the transfection in HepG2.2.15 cells could be inhibited by pretreating the cells with galactose [30]. Also, the distribution of ^{3}H-labelled SG cationic liposomes in rat hepatocytes was higher than that of non-SG liposomes [17]. Furthermore, transfection of SG-liposomes as gene delivery carrier in HepG2 cells was more efficient than in HeLa human cervix carcinoma cells, 293 human kidney epithelial cells and Y1 mouse hormone-secreting adrenal cortex cells [31]. Hwang et al. suggested that the cationic liposomes containing sito-G on the liposomes surface brought significant improvement to the transfection efficiency in HepG2 cells and attributed this improvement to the ASGPR recognition to sito-G [16], but provided no direct evidence about receptor binding test. Asialofetuin or galactosylated albumin were often used to evaluate the hepatocyte-targeting effect via ASGPR in vitro or in vivo, because they could bind to ASGPR specifically and thus block the receptor completely. In the presence of asialofetuin or galactosylated albumin the hepatocyte-targeting effect would be inhibited completely and the transfection efficiency would also be decreased [32–34]. In this study, the modification with sito-G in the cationic liposomes (CL/sito-G and CL/Brij 35/sito-G) enhanced the transfection efficiency and improved the antigens inhibition effect in vitro. Moreover, the receptor binding competition test with asialofetuin suggested that the improvement was dependent on the ASGPR-mediated pathway, which meant that sito-G would be a useful ligand in the ASGPR-mediated hepatocyte-targeting.

Endocytosis and membrane fusion were the major pathways of the asODN cellular uptake, and the former was usually the primary step in the efficient gene transfection. Noguchi et al. suggested that either wortmannin (endocytosis) or nigericin (membrane fusion) might completely inhibit the asODN transfection, because membrane fusion was the subsequent step upon endocytosis [35]. In our experiments, as for the co-modified cationic liposomes, both wortmannin and nigericin partly inhibited the asODN transfection, which suggested that there might be some cellular uptake pathways for the co-modified cationic liposomes other than endocytosis and

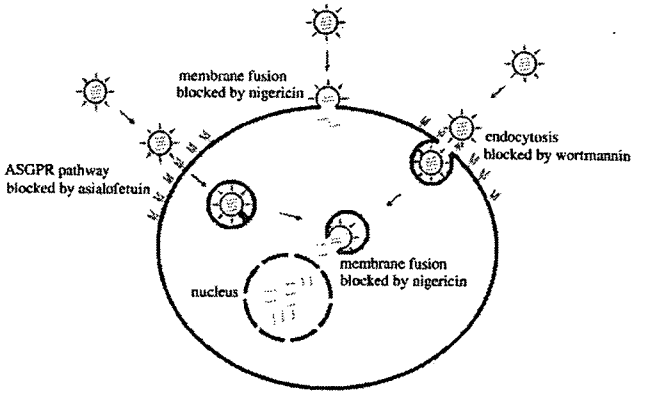

Fig. 9. A schematic representation shows the cellular uptake and delivery of asODN from CL/brij35/sito-G in hepatocytes. Endocytosis pathway: the liposomes were taken up by the membrane endocytosis with endosomes formed and then asODN was released by membrane fusion between the endosomes and the liposomes. ASGPR pathway: the liposomes were taken up based on the specific recognition of the ligand sito-G by ASGPR and the endosome was formed. Membrane fusion pathway: asODN was released into the cytoplasm at the membrane by the fusion between cell membrane and liposome membrane. After being released, most of the asODN would be accumulated into the nuclear.

membrane fusion in endosomes. For example, fusion might also occur between liposomes and cell membrane and the asODN would be released across the cell membrane, because Brij 35 could destabilize the cell membrane as the nonionic surfactant and thus induce the lipid exchange between liposomes and cell membrane [18]. Different lipids and cell types could result in different cellular uptake processes of the cationic liposomes, as reviewed by Duzgune and Nir [19]. As reported previously, phosphatidylcholine (PC) like DPPC was generally inhibitory to membrane fusion while phosphatidylethanolamine (PE) like DOPE could facilitate it, and consequently, PE-cationic liposomes showed more efficient transfection than PC-cationic liposomes [19]. In this study, although containing DPPC as co-lipid, the cationic liposomes resulted in membrane fusion in endosomes. Considering that Brij 35 has a long oxyethylene chain which would destabilize the endosome membrane [18] and a long alkyl chain which might improve the fluidity of cationic liposomes, it could be presumed that it was the addition of Brij 35 that improved the transmembrane ability of the cationic liposomes by fusion process. Kim et al. also reported that Tween 80 could enhance "lipofection" of the emulsion–DNA complexes, and presumed that Tween 80 had the fusogenic property [18]. Besides, sito-G might also contribute partly to the membrane fusion because of its penetration-enhancing effect [16].

With the help of several inhibitors acting on different steps for the encapsulated asODN to be delivered into the cells, the cellular uptake mechanisms of the encapsulated asODN in CL/Brij 35/sito-G (Fig. 9) were concluded to be a complicated process which involved at least endocytosis, membrane fusion and ASGPR-mediated pathway (also endocytosis). Sito-G showed to be a useful ligand in the liver-targeting gene delivery, and Brij 35 seemed to be able to facilitate the membrane fusion in the lipofection. Based on this conclusion, it might be most meaningful for combining the ligand with the nonionic surfactant in the oriented delivery of asODN to optimize the transfection in vivo, because the enhanced endocytosis by the ligand, and the facilitated delivery from the endosomes by the nonionic surfactant, would be achieved at the same time. If necessary, some bio-surfactants that may be safer could be used to substitute Brij 35 in vivo.

Acknowledgement

This work was supported by the National Natural Science Foundation of China, 30371265 and 90406024.

References

[1] S. Akhtar, M.D. Hughes, A. Khan, M. Bibby, M. Hussain, Q. Nawaz, J. Double, P. Sayyed, The delivery of antisense therapeutics, Adv. Drug Deliv. Rev. 44 (2000) 3–21.

[2] J. Weyermann, D. Lochmann, A. Zimmer, Comparison of antisense oligonucleotide drug delivery systems, J. Control. Release 100 (2004) 411–423.

[3] D.C. Litzinger, J.M. Brown, I. Wala, S.A. Kaufman, G.Y. Van, C.L. Farrell, D. Collins, Fate of cationic liposomes and their complex with oligonucleotide in vivo, Biochim. Biophys. Acta 1281 (1996) 139–149.

[4] M.C. Woodle, P. Scaria, Cationic liposomes and nucleic acids, Curr. Opin. Colloid Interface Sci. 6 (2001) 78–84.

[5] C. Guha, S.J. Shah, S.S. Ghosh, S.W. Lee, N. Roy-Chowdhury, J. Roy-Chowdhury, Molecular therapies for viral hepatitis, Biodrugs 17 (2003) 81–91.

[6] R. Xu, K. Cai, D. Zheng, H. Ma, S. Xu, S.T. Fan, Molecular therapeutics of HBV, Curr. Gene Ther. 3 (2003) 341–355.

[7] B.E. Korba, J.L. Gerin, Antisense oligonucleotides are effective inhibitors of hepatitis B virus replication in vitro, Antivir. Res. 28 (1995) 225–242.

[8] Z. Yao, Hepatitis B Virus-associated Molecular Epidemiology, Chinese Medical Science and Technology Press, Beijing, China, 1994.

[9] M. Singh, M. Ariatti, Targeted gene delivery into HepG2 cells using complexes containing DNA, cationized asialoorosomucoid and activated cationic liposomes, J. Control. Release 92 (2003) 383–394.

[10] H. Hirabayashi, M. Nishikawa, Y. Takakura, M. Hashida, Development and pharmacokinetics of galactosylated poly-L-glutamic acid as a biodegradable carrier for liver-specific drug delivery, Pharm. Res. 13 (1996) 880–884.

[11] P. Kallinteri, W.Y. Liao, S.G. Antimisiaris, K.H. Hwang, Characterization, stability and in-vivo distribution of asialofetuin glycopeptide incorporating DSPC/CHOL liposomes prepared by mild cholate incubation, J. Drug Target. 9 (2001) 155–168.

[12] H.H. Spanjer, G.L. Scherphof, Targeting of lactosylceramide-containing liposomes to hepatocytes in vivo, Biochim. Biophys. Acta 734 (1983) 40–47.

[13] S.R. Popielarski, S. Hu-Lieskovan, S.W. French, T.J. Triche, M.E. Davis, A nanoparticle-based model delivery system to guide the rational design of gene delivery to the liver. 2. In vitro and in vivo uptake results, Bioconjug. Chem. 16 (2005) 1071–1080.

[14] K. Shimizu, X.R. Qi, Y. Maitani, M. Yoshie, K. Kawano, K. Takayama, T. Nagai, Targeting of soybean-derived sterylglucoside liposomes to liver tumors in rat and mouse models, Biol. Pharm. Bull. 21 (1998) 741–746.

[15] K. Kawano, K. Nakamura, K. Hayashi, T. Nagai, K. Takayama, Y. Maitani, Liver targeting liposomes containing beta-sitosterol glucoside with regard to penetration-enhancing effect on HepG2 cells, Biol. Pharm. Bull. 25 (2002) 766–770.

[16] S.H. Hwang, K. Hayashi, K. Takayama, Y. Maitani, Liver-targeted gene transfer into a human hepatoblastoma cell line and in vivo by sterylglucoside-containing cationic liposomes, Gene Ther. 8 (2001) 1276–1280.

[17] J. Shi, W.W. Yan, X.R. Qi, Y. Maitani, T. Nagai, Characteristics and biodistribution of soybean sterylglucoside and polyethylene glycol-modified cationic liposomes and their complexes with antisense oligodeoxynucleotide, Drug Deliv. 12 (2005) 349–356.

[18] T.W. Kim, Y.J. Kim, H. Chung, I.C. Kwon, H.C. Sung, S.Y. Jeong, The role of non-ionic surfactants on cationic lipid mediated gene transfer, J. Control. Release 82 (2002) 455–465.

[19] N. Duzgune, S. Nir, Mechanisms and kinetics of liposome-cell interactions, Adv. Drug Deliv. Rev. 40 (1999) 3–18.

[20] W.W. Yan, R. Fei, W. Wang, X.R. Qi, L. Wei, X. Cong, Y. Wang, Influence of soybean-derived sterylglucoside and amphipathic polyethylene glycol on the cellular delivery and anisotropy of different cationic liposomes, J. Peking Univ. [Health Sci.] 35 (2003) 324–328.

[21] P.O. Seglen, Preparation of isolated rat liver cells, Methods Cell Biol. 13 (1976) 29–83.

[22] S.W. Yi, T.Y. Yun, T.W. Kim, H. Chung, Y.W. Choi, I.C. Kwon, E.B. Lee, S.Y. Jeong, A cationic lipid emulsion–DNA complex as a physically stable and serum-resistant gene delivery system, Pharm. Res. 17 (2000) 314–320.

[23] M. Nakanishi, A. Noguchi, Confocal and probe microscopy to study gene transfection mediated by cationic liposomes with a cationic cholesterol derivative, Adv. Drug Deliv. 52 (2001) 197–207.

[24] M. Robaczewska, S. Guerret, J.S. Remy, I. Chemin, W.B. Offensperger, M. Chevallier, J.P. Behr, A.J. Podhajska, H.E. Blum, C. Trepo, L. Cova, Inhibition of hepadnaviral replication by polyethylenimine-based intravenous delivery of antisense phosphodiester oligodeoxynucleotides to the liver, Gene Ther. 8 (2001) 874–881.

[25] P.N. Soni, D. Brown, R. Saffie, K. Savage, D. Moore, G. Gregoriadis, G.G. Dusheiko, Biodistribution, stability, and antiviral efficacy of liposome-entrapped phosphorothioate antisense oligodeoxynucleotides in ducks for

the treatment of chronic duck hepatitis B virus infection, Hepatology 28 (1998) 1402–1410.
[26] S. Agrawal, Importance of nucleotide sequence and chemical modifications of antisense oligonucleotides, Biochim. Biophys. Acta 1489 (1999) 53–68.
[27] G.L. Lukacs, P. Haggie, O. Seksek, D. Lechardeur, N. Freedman, A.S. Verkman, Size-dependent DNA mobility in cytoplasm and nucleus, J. Biol. Chem. 275 (2000) 1625–1629.
[28] F. Shi, W.H. Visser, D.N.M.J. Jong, R.S.B. Liem, E. Ronken, D. Hoekstra, Antisense oligonucleotides reach mRNA targets via the RNA matrix; downregulation of the 5-HT1A receptor, Exp. Cell Res. 291 (2003) 313–325.
[29] W.T. Godbey, K.K. Wu, A.G. Mikos, Tracking the intracellular path of poly(ethylenimine)/DNA complexes for gene delivery, Proc. Natl. Acad. Sci. U. S. A. 96 (1999) 5177–5181.
[30] J. Shi, X.R. Qi, L. Yang, R. Fei, L. Wei, Liver targeting of cationic liposomes modified with soybean-derived sterylglucoside in vitro, Acta Pharm. Sin. 41 (2006) 19–23.
[31] Y. Maitani, S.H. Hwang, S. Tanaka, K. Takayama, T. Nagai, Physicochemical characteristics and transfection efficiency of DNA in liposomes with soybean-derived sterylglucoside into HepG 2 cells, J. Pharm. Sci. Technol. Jpn. 61 (2001) 1–10.
[32] Y. Maitani, K. Kawano, K. Yamada, T. Nagai, K. Takayama, Efficiency of liposomes surface-modified with soybean-derived sterylglucoside as a liver targeting carrier in HepG2 cells, J. Control. Release 75 (2001) 381–389.
[33] T. Niidome, M. Urakawa, H. Sato, Y. Takahara, T. Anai, T. Hatakayama, A. Wada, T. Hirayama, H. Aoyagi, Gene transfer into hepatoma cells mediated by galactose-modified alpha-helical peptides, Biomaterials 21 (2000) 1811–1819.
[34] M. Nishikawa, M. Yamauchi, K. Morimoto, E. Ishida, Y. Takakura, M. Hashida, Hepatocyte-targeted in vivo gene expression by intravenous injection of plasmid DNA complexed with synthetic multi-functional gene delivery system, Gene Ther. 7 (2000) 548–555.
[35] A. Noguchi, T. Furuno, C. Kawaura, M. Nakanishi, Membrane fusion plays an important role in gene transfection mediated by cationic liposomes, FEBS Lett. 433 (1998) 169–173.

DNA/Lipid Complex Incorporated with Fibronectin to Cell Adhesion Enhances Transfection Efficiency in Prostate Cancer Cells and Xenografts

Yoshiyuki HATTORI and Yoshie MAITANI*

Institute of Medicinal Chemistry, Hoshi University; 2–4–41 Ebara, Shinagawa-ku, Tokyo 142–8501, Japan.
Received August 19, 2006; accepted December 20, 2006; published online December 22, 2006

Previously we have described the development and applications of lipid-based nanoparticles for gene delivery vector. In an attempt to improve transfection efficiency using the cell adhesion of extracellular matrix (ECM) to DNA/lipid complex (nanoplex), the mRNA expression of integrin $\alpha 2\beta 1$ and CD44 in prostate cancer cells was detected as adhesion molecules for fibronectin (Fn), collagen I (Col) and laminin (Lam) using a commercially available cDNA array (GEArray™) system. These ECM proteins could enhance DNA transfection activity in cells when coated on the nanoplex. Among the ECM proteins, Fn-coating nanoplexes significantly increased transfection activity 2-fold in prostate cancer PC-3 cells, and exhibited higher DNA transfection activities to PC-3 xenografts, compared with commercially available cationic polymer *in vivo* jetPEI. These results indicated that Fn-coating nanoplexes could facilitate efficient transfection of prostate tumor cells.

Key words adhesion molecule; prostate tumor; nanoparticle; transfection; fibronectin; collagen I

Extracellular matrix (ECM) consists of a group of well-characterized glycoproteins, which are present at the epithelial-mesenchymal interface of both begin and malignant tissues.[1] Tumor cell adhesion to ECM components such as fibronectin (Fn), laminin (Lam) and collagen 1 (Col) is mediated *via* integrin subunits, and ECM components play a major role in the invasion and metastasis of tumor cells.[2]

ECM protein and adhesion molecules have been used for tumor gene delivery. The arginin–glycine–aspartic acid (RGD) sequence is well known to serve as a recognition motif in multiple ligands for several different integrins such as integrin $\alpha v\beta 3$ and $\alpha 5\beta 1$ *et al.*[3] RGD-modified liposomes[4,5] and polymers[6,7] have been developed as gene transfer vectors. An electrostatic complex consisting of a cationic liposome, an integrin $\alpha 5\beta 1$-targeting peptide, and plasmid DNA, was efficiently vector transfected to tumor cells.[8,9] Recently, it has been reported that calcium phosphate/DNA complex with ECM proteins, especially Col and Fn, led to remarkably high transgene expression in mammalian cells.[10] Cells can attach to ECM proteins *via* plasma membrane receptor proteins. Therefore, ECM proteins for adhesion to tumor cells can be useful for gene delivery to increase gene expression by enhancing the association of genes with cells. However, no attention was paid to the complexation of lipid-based cationic liposomes or nanoparticles with ECM proteins.

Lipid-based cationic nanoparticles could deliver DNA with significantly high transfection efficiency into prostate tumor cells.[11] To improve nanoparticle-mediated transfection for *in vivo* application, the effect of cell adhesion of nanoplex on gene transfer efficiency was investigated. First, mRNA expression of integrin $\alpha 2\beta 1$ and CD44 in prostate cancer cells was detected as adhesion molecules for Fn, Col and Lam using a commercially available cDNA array (GEArray™) system. Second, we prepared a ternary complex of the nanoparticle/DNA complex (nanoplex) with Fn, Col and Lam (Fn, Col and Lam nanoplex) and evaluated transfection activity in PC-3 cells and xenografts.

MATERIALS AND METHODS

Cell Culture Prostate tumor LNCaP and PC-3 cells were supplied by the Cell Resource Center for Biomedical Research, Tohoku University (Miyagi, Japan). The cells were grown in a RPMI-1640 medium (Life Technologies, Inc., Grand Island, NY, U.S.A.) supplemented with 10% heat-inactivated fetal bovine serum (FBS) (Life Technologies, Inc.) and kanamycin (100 μg/ml) at 37 °C in a 5% CO_2 humidified atmosphere.

Cell Spreading For coating Fn, Col and Lam onto tissue culture dishes, Fn (human fibronectin, BD Bioscience, Bedford, MA, U.S.A.), Col (human collagen I, Morinaga Institute of Biological Science, Yokohama, Japan) and Lam (mouse laminin, Harbor Bio-Products, Norwood, MA, U.S.A.), respectively, were diluted to 50 μg/ml with PBS (pH 7.4), and added to 35 mm tissue culture dishes. The plates were incubated for 1 h at 37 °C. After coating the plates, they were washed 3 times in PBS, and were plated 1×10^6 PC-3 or LNCaP cells in RPMI-1640 medium onto the dishes. After 3 h incubation, the unattached cells were removed by exchanging the medium, and the attached cells on the dishes were examined microscopically for the number of spread cells.

cDNA Array Total RNA from LNCaP or PC-3 cells was extracted using the RNasy mini kit (Qiagen, Hilden, Germany). Non-radioactive human extracellular matrix and an adhesion molecule gene array (Super Array, Inc., MD, U.S.A.) were used to analyze the gene expression profile of extracellular matrix and adhesion molecules according to the manufacturer's protocol. The results were analyzed using free ScanAlyze software (developed by Dr. Michael Eisen), which converts a grayscale TIFF image of spots into numerical data (median pixel intensity), and then the gene expression profiles were compared using GEArray analyzer software (Super Array, Inc.). Normalized intensities were calculated from each array by subtracting the negative control from each spot.

Preparation of Plasmid DNA The plasmid pCMV-luc encoding the luciferase gene under the control of the CMV

* To whom correspondence should be addressed. e-mail: yoshie@hoshi.ac.jp

promoter was constructed as previously described.[12] A protein-free preparation of these plasmids was purified following alkaline lysis using maxiprep columns (Qiagen).

Preparation and Size Measurement of Nanoparticles and Nanoplexes Cholesteryl-3β-carboxyamidoethylene-*N*-hydroxyethylamine (OH-Chol) was synthesized as previously described.[11] Tween 80 was obtained from NOF Co., Ltd. (Tokyo, Japan). Lipid-based nanoparticles were prepared with lipids (OH-Chol : Tween 80=10 : 1.3 mg) in 10 ml water by the modified ethanol injection method as previously described.[11] The nanoplex at a charge ratio (+/−) of cationic lipid to DNA of 3/1 was formed by the addition of 9.5 μl of the nanoparticle solution to 2 μg DNA in 50 μl of 50 mM NaCl solution with gentle shaking and leaving at room temperature for 10 min. To prepare ternary complexes with ECM protein (Fn, Col and Lam nanoplex), the nanoplex with 2 μg DNA was mixed with 2 or 5 μg of Fn, Col and Lam, respectively, and incubated for 10 min. The particle size distributions and ζ-potentials were measured by the dynamic light scattering method and the electrophoresis light scattering method, respectively (ELS-800, Otsuka Electronics Co., Ltd., Osaka, Japan), at 25 °C after the dispersion was diluted to an appropriate volume with water.

Luciferase Assay For transfection, Fn, Col and Lam nanoplexes, respectively, were diluted in 1 ml of medium supplemented with 10% FBS and then incubated for 24 h. Lipofectamine 2000 (Invitrogen Corp., Carlsbad, CA, U.S.A.) lipoplex at a charge ratio (+/−) of 2/1 of cationic lipid to DNA was prepared according to the manufacturer's protocol. Luciferase expression was measured as counts per second (cps)/μg protein using the luciferase assay system (Pica gene, Toyo Ink Mfg. Co., Ltd., Tokyo, Japan) and BCA reagent (Pierce, Rockford, IL, U.S.A.) as previously reported.[13]

Cell Viability The cell viabilities upon transfection using Fn, Col and Lam nanoplex were evaluated with a cell proliferation assay kit (Dojindo, Kumamoto, Japan). Cells were placed in a 96-well plate in the medium containing serum, and were transfected with nanoplex of 0.2 μg plasmid DNA with ECM protein (0.2 μg). After 24 h of incubation, the cell viabilities were measured according to the manufacturer's protocol.

***In Vivo* Transfection** To generate PC-3 tumor xenografts, 1×10^7 cells suspended in 50 μl of RPMI medium were inoculated subcutaneously into the flank of male BALB/c nu/nu mice (7 weeks of age, CLEA Japan, Inc., Tokyo, Japan). To prepare Fn nanoplex, the nanoplex with 10 μg DNA at a charge ratio (+/−) of cationic lipid to DNA of 3/1 was mixed with 10 μg of Fn as described above section. The Fn nanoplex was administered to the xenografts with a tumor volume of about 200—300 mm^3 by intratumoral injection (10 μg of plasmid DNA/tumor) as previously reported.[14] *In vivo* jetPEI, a commercially available cationic polymer transfection reagent (PolyPlus-transfection, Llkirch, France), was used according to the manufacturer's protocol for *in vivo* administration. Twenty-four hours after injection, D-luciferin (potassium salt) dissolved in PBS (125 mg/kg of body weight) was injected into the mouse peritoneal cavity (i.p.) and subsequently anesthetized by i.m. injection of 50 mg/kg body weight of pentobarbital (Nembutal, Dainippon Pharmaceutical Co., Ltd., Osaka, Japan). *In vivo* bioluminescence imaging was performed using an NightOWL LB981 NC100 system (Berthold Technologies, Bad Wildbad, Germany). A gray scale body-surface reference image was collected using a NightOWL LB981 CCD camera. Photons emitted from luciferase within the mice and transmitted through its tissues were collected and integrated for a 2 min period. Overlay of the real image and luminescence representation allowed the localization and measurement of luminescence emitted from xenografts. The signal intensities from manually derived regions (ROI) of interest were obtained and data were expressed as photon flux (count/s). Background photon flux was defined from an ROI of the same size placed in a nonluminescent area near the mice and then subtracted from the measured luminescent signal intensity.

Statistical Analysis Data were compared using analysis of variance and evaluated by Student's *t* test or Welch's *t* test. A *p* value of ≤0.05 was considered significant.

RESULTS AND DISCUSSION

Previously we reported that a lipid-based nanoparticle composed of OH-Chol as a cationic lipid showed significantly high transfection efficiency into prostate tumor cells when complexed with plasmid DNA in the presence of 50 mM NaCl solution.[11] In this study, we improved this nanoparticle by coating ECM proteins onto nanoplex to enhance transfection activity into PC-3 and LNCaP cells. LNCaP and PC-3 are prostate cancer cell lines with low and high metastatic potential, respectively.[15]

First, we tested three different ECM proteins for their cell adhesion to a plastic surface. In PC-3 cells, cell adhesion was increased by coating with Fn, Col and Lam (Fig. 1A), but in LNCaP cells, it was only slightly increased by coating with Fn (Fig. 1B). These results indicated that ECM proteins could strongly associate with adhesion molecules on the cell surface of high metastatic PC-3 cells compared with low metastatic LNCaP cells.

To identify which adhesion molecule on the cell surface of a prostate tumor promoted adhesion with ECM protein-coating plates, we utilized a commercially available ECM and adhesion molecule-specific cDNA array (GEArray™) system for the analysis of 96 genes (Table 1). In PC-3 cells, strong mRNA expression was observed for 2 genes, CD44 and catenin β1, moderate mRNA expression for 4 genes, integrin β1, hyaluronidases, PECAM-1 and maspin, weak mRNA expression for 7 genes, Meth, E-cadherin, CEA, catenin delta 1, cathepsin L, fibronectin 1 and integrin α2. In LNCaP cells, strong mRNA expression was observed for 5 genes, Meth, CEA, catenin β1, catenin delta 1 and hyaluronidases, moderate mRNA expression for 2 genes, E-cadherin and integrin β1, and weak mRNA expression for 3 genes, cathepsin L, fibronectin 1 and maspin. We found the mRNA expression of CD44 and integrin $\alpha2\beta1$ for the receptors of Fn, Col or Lam in PC-3 cells, but not in LNCaP cells. These expression profiles in genes corresponded with previous studies[16,17] and confirmed that the adhesion of PC-3 cells to the tissue culture plate was increased by coating with ECM proteins than that of LNCaP cells (Fig. 1).

Next, we prepared nanoplex coating with ECM proteins and evaluated transfection activity into PC-3 and LNCaP cells. The average size of non-coated nanoparticle was approximately 120—130 nm with about +50 mV of ζ-poten-

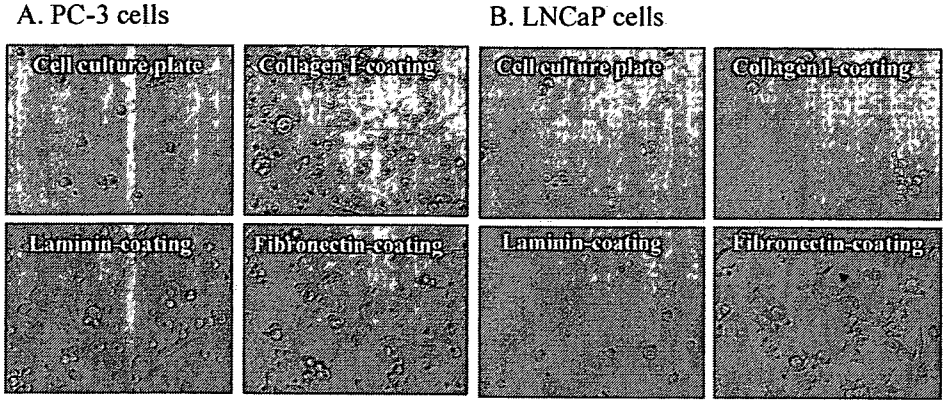

Fig. 1. Photomicrografts of PC-3 (A) and LNCaP (B) Plated on a Cell Culture Plate Coated with ECM Protein
Cells were incubated for 1 h with non-coated, Fn-, Col- or Lam-coated tissue culture palates. Magnification ×200.

Table 1. Differential Expression of Genes in PC-3 and LNCaP Cells

Gene name	PC-3	LNCaP
Meth	+	+++
CD44	+++	−
E-cadherin	+	++
CEA	+	+++
Catenin β1	+++	+++
Catenin delta1	+	+++
Cathepsin L	+	+
Fibronectin 1	+	+
Integrin α2	+	−
Integrin β1	++	++
Hyaluronidases	++	+++
PECAM-1	++	−
Maspin	++	+

This table shows the optical density of the spot in cDNA array. Median pixel intensity of each spot in cDNA array was calculated using ScanAlyze software, which is a program for DNA microarray imaging and extracts median pixel intensity (range: 0—65536) from the image data of spots. +++: pixel intensity >25000, ++: 25000—15000, +: 15000—5000, −: <5000.

tial, and the size of non-coated nanoplex mixed with 2 μg plasmid DNA and the nanoparticle increased to 800 nm (about +39 mV of ζ-potential). In ECM protein-coated nanoplexes, their size depended on ECM protein. When the nanoplex of 2 μg plasmid DNA was complexed with 2 μg of Fn and Col, the sizes of Fn and Col nanoplexes decreased to approximately 230 and 430 nm, respectively, and their ζ-potential decreased to −16.3 and +8.0 mV, respectively, suggested Fn and Col coating on nanoplexes. In contrast, when the nanoplex of 2 μg plasmid DNA was complexed with 2 μg of Lam, the size of the Lam nanoplex was greatly increased in size (11 μm) and ζ-potential was decreased to +14.2 mV. It was not clear why the size of the nanoplex decreased after mixing with Fn and Col.

We examined the effect of ECM proteins on the transfection mediated by the nanoplexes. Enhanced transfection was observed when 2 μg of Fn and Lam was associated with nanoplexes of 2 μg plasmid DNA (Fig. 2A). Two and five micrograms of these proteins showed a similar level of luciferase gene expression, indicating that 2 μg of ECM proteins were sufficient for transfection. In LNCaP cells, transfection efficiency was slightly increased by coating with Fn or Col, but not significantly compared to the non-coated nanoplex (Fig. 2B). Fn, Col and Lam nanoplexes exhibited slightly decrease of cell viabilities (74, 86 and 85%, respectively, compared with that of non-coated nanoplex (89%)) (data not shown). Many parameters including size of nanoplex are known to affect transfection efficiency.[18,19] Large lipoplexes over 700 nm in mean diameter induced efficient transfection than lipoplexes with 250 nm.[20] The size of Lam nanoplex (11 μm) was greatly larger than that of Fn and Col nanoplexes; therefore, Lam nanoplex might increase gene transfer efficiency in PC-3 cells.

Our results demonstrated that the association of Fn with cationic nanoplex produced a ternary complex, which showed much higher transfection activity into PC-3 cells. Fn is a large (440 kDa) multidomain extracellular matrix protein with an RGD site that is not exposed in its native compact conformation. Fn adopts a conformation that is more open than its compact conformation when bound to liposome vector.[21] This open confirmation exposes a hidden RGD site in Fn that stimulates binding to adhesion molecules.[21] In our study, the hidden RGD site of the Fn nanoplex might be exposed. CD44 expression was seen in PC-3 cells but not LNCaP cells. CD44 can bind to Col, Fn and Lam,[22] and the ligands of integrin $\alpha 2\beta 1$ are Lam and Col.[23] This suggested that Fn nanoplex was likely to bind mainly to CD44, and to increase the association of nanoplex with the cells, resulting in enhanced transfection efficiency in PC-3 cells.

Among ECM-coated nanoplexes, the Fn nanoplex (2 μg Fn for 2 μg plasmid DNA) was injectable in size (230 nm) and increased transfection efficiency in PC-3 cells, being comparable to lipofectamine 2000. Therefore, we decided to use Fn nanoplex for *in vivo* gene delivery by direct injection into PC-3 tumor xenografts. As a control, we used commercially available transfection polymer *in vivo* jetPEI, because non-coated nanoplex was not injectable in size. To analyze the level of luciferase expression, we imaged mice and quantified bioluminescence using an NightOWL LB981 NC100 system, expressed as photon/s/tumor. Figure 3 shows the efficiency of Fn nanoplex (10 μg Fn for 10 μg plasmid DNA) to carry DNA into PC-3 tumor xenografts in nude mice. Fn nanoplex showed significantly 4-fold more efficient transfection activity than *in vivo* jetPEI (Figs. 3A, B). This finding suggested that Fn proteins with exposed conformation could effectively interact with the corresponding receptors, allowing the strong induction of expression in metastatic prostate tumor. Considering the simplicity, level of efficiency, and

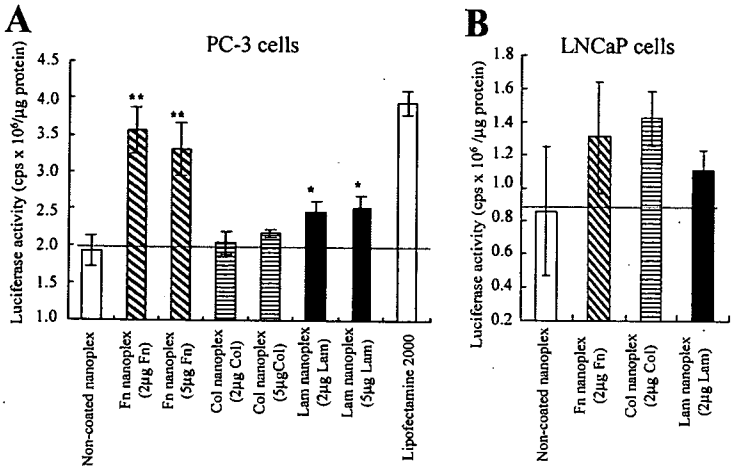

Fig. 2. The Effect of ECM Protein Complexed with Nanoplex on Luciferase Gene Expression in PC-3 (A) and LNCaP (B) Cells

The nanoplex of 2 μg plasmid DNA was complexed with 2 μg or 5 μg of Fn, Col or Lam. $*p<0.05$, $**p<0.01$ compared with non-coated nanoplex.

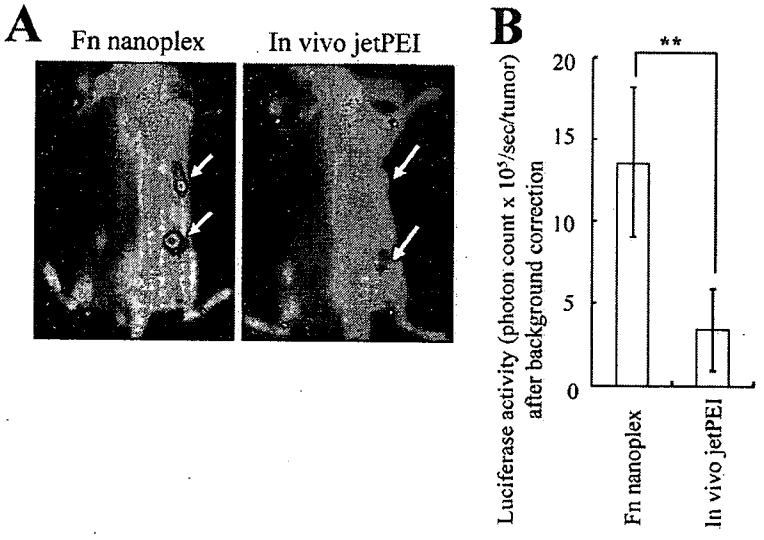

Fig. 3. Tumor Transfection *in Vivo*

Xenografts of PC-3 tumor cells were directly injected with 10 μg plasmid DNA by Fn nanoplex (Fn 10 μg) and *in vivo* jetPEI polyplex, respectively. Arrowheads indicate solid tumor injected DNA into xenografts. Twenty-four hours after i.t. injections, mice were imaged and bioluminescence was quantified. A shows pseudocolor luminescent images from blue (least intense) to red (most intense), representing light emitted from tumors superimposed over a grayscale reference image of representative mice from each group of three. B. Quantification of emitted photons from each tumor. $**p<0.01$ compared with Fn nanoplex.

minimal cost, this technique emerges as a valuable tool for gene delivery.

In conclusion, we focused on the alternation of ECM and adhesion molecules in the progression of prostate cancer, and found that Fn-coated nanoplex increased transfection efficiency in metastatic prostate tumor. These results indicated that extracellular matrix-coated nanoplex could facilitate the efficient transfection of prostate tumor cells.

Acknowledgements This project was supported in part by a grant from the Promotion and Mutual Aid Corporation for Private Schools of Japan, and by a Grant-in-Aid for Scientific Research from the Ministry of Education, Culture, Sports, Science and Technology of Japan.

REFERENCES

1) Scott G., Cassidy L., Busacco, A., *J. Invest Dermatol.*, **108**, 147—153 (1997).
2) Saiki I., *Jpn. J. Pharmacol.*, **75**, 215—242 (1997).
3) Romanov V. I., Goligorsky M. S., *Prostate*, **39**, 108—118 (1999).
4) Anwer K., Kao G., Rolland A., Driessen W. H., Sullivan S. M., *J. Drug Target*, **12**, 215—221 (2004).
5) Harvie P., Dutzar B., Galbraith T., Cudmore S., O'Mahony D., Anklesaria P., Paul R., *J. Liposome Res.*, **13**, 231—247 (2003).
6) Schiffelers R. M., Ansari A., Xu J., Zhou Q., Tang Q., Storm G., Molema G., Lu P. Y., Scaria P. V., Woodle M. C., *Nucleic Acids Res.*, **32**, e149 (2004).
7) Kunath K., Merdan T., Hegener O., Haberlein H., Kissel T., *J. Gene Med.*, **5**, 588—599 (2003).
8) Jenkins R. G., Meng Q. H., Hodges R. J., Lee L. K., Bottoms S. E., Laurent G. J., Willis D., Ayazi S. P., McAnulty R. J., Hart S. L., *Gene Ther.*, **10**, 1026—1034 (2003).
9) Hart S. L., Arancibia-Carcamo C. V., Wolfert M. A., Mailhos C., O'Reilly N. J., Ali R. R., Coutelle C., George A. J., Harbottle R. P.,

Knight A. M., Larkin D. F., Levinsky R. J., Seymour L. W., Thrasher A. J., Kinnon C., *Hum. Gene Ther.*, **9**, 575—585 (1998).
10) Chowdhury E. H., Nagaoka M., Ogiwara K., Zohra F. T., Kutsuzawa K., Tada S., Kitamura C., Akaike T., *Biochemistry*, **44**, 12273—12278 (2005).
11) Hattori Y., Kubo H., Higashiyama K., Maitani Y., *J. Biomed. Nanotech.*, **1**, 176—184 (2005).
12) Igarashi S., Hattori Y., Maitani Y., *J. Control Release*, **112**, 362—368 (2006).
13) Hattori Y., Maitani Y., *Cancer Gene Ther.*, **12**, 796—809 (2005).
14) Hattori Y., Maitani Y., *Cancer Sci.*, **97**, 787—798 (2006).
15) Aalinkeel R., Nair M. P., Sufrin G., Mahajan S. D., Chadha K. C., Chawda R. P., Schwartz S. A., *Cancer Res.*, **64**, 5311—5321 (2004).
16) Dhir R., Gau J. T., Krill D., Bastacky S., Bahnson R. R., Cooper D. L., Becich M. J., *Mol. Diagn.*, **2**, 197—204 (1997).
17) Kostenuik P. J., Sanchez-Sweatman O., Orr F. W., Singh G., *Clin. Exp. Metastasis*, **14**, 19—26 (1996).
18) Almofti M. R., Harashima H., Shinohara Y., Almofti A., Li W., Kiwada H., *Mol. Membr. Biol.*, **20**, 35—43 (2003).
19) Escriou V., Ciolina C., Lacroix F., Byk G., Scherman D., Wils P., *Biochim. Biophys. Acta*, **1368**, 276—288 (1998).
20) Turek J., Dubertret C., Jaslin G., Antonakis K., Scherman D., Pitard B., *J. Gene Med.*, **2**, 32—40 (2000).
21) Halter M., Antia M., Vogel V., *J. Control Release*, **101**, 209—222 (2005).
22) Goodison S., Urquidi V., Tarin D., *Mol. Pathol.*, **52**, 189—196 (1999).
23) Fornaro M., Manes T., Languino L. R., *Cancer Metastasis Rev.*, **20**, 321—331 (2001).

Combination of non-viral connexin 43 gene therapy and docetaxel inhibits the growth of human prostate cancer in mice

MASAYOSHI FUKUSHIMA, YOSHIYUKI HATTORI, TAKASHI YOSHIZAWA and YOSHIE MAITANI

Institute of Medicinal Chemistry, Hoshi University, Shinagawa-ku, Tokyo 142-8501, Japan

Received August 24, 2006; Accepted November 23, 2006

Abstract. Docetaxel (DTX) is used for the treatment of advanced hormone refractory prostate cancer. Connexin 43 (Cx43) is a tumor suppressor gene, and transfection of the Cx43 gene increases sensitivity to several chemotherapeutic agents. The objective of this study was to evaluate the effectiveness of combination therapy of Cx43-expressing plasmid DNA (pCMV-Cx43) and DTX both *in vitro* and *in vivo* using a non-viral vector in human prostate cancer PC-3 cells. Transfection of pCMV-Cx43 into the cells neither inhibited tumor growth nor increased gap junctional intercellular communication; however, combination therapy of pCMV-Cx43 and DTX significantly inhibited cell growth. Forced expression of Cx43 in the cells induced apoptotic cells by down-regulation of Bcl-2 expression and significantly more up-regulation of caspase-3 activity than either treatment alone. The combination of repeated intratumoral injection of pCMV-Cx43 (10 μg/tumor) with non-viral vector and a single intravenous injection of DTX (15 mg/kg) was compared with a repeated injection of Cx43 alone and a single injection of DTX alone on PC-3 tumor xenografts. Significant antitumoral effects were observed in mice receiving combined treatment, compared with DTX alone. The data presented here provide a rational strategy for treating patients with advanced hormone refractory prostate cancer.

Introduction

Prostate cancer is a significant problem and is reported to be the leading cancer diagnosed in man (1). Cytotoxic chemotherapy has shown significant palliative benefit in the treatment of androgen-independent prostate cancer, but with no survival advantage demonstrated to date (2). Current chemotherapy is limited by drug tolerance and the ultimate emergence of resistant disease (3). Novel approaches incorporating potentially more active and less toxic agents that may overcome drug resistance mechanisms need to be investigated. Increased understanding of the tumor biology of prostate cancer offers promise of novel treatments for this disease.

Docetaxel (DTX), a member of the taxane family, is semisynthesized from an inactive taxoid precursor extracted from the needles of the European yew, *Taxus baccata*. DTX has shown clinical activity in a wide spectrum of solid tumors including breast, lung, ovarian, and prostate cancers (4,5). The known basic cellular target of DTX is the microtubule. Furthermore, DTX down-regulates genes for cell proliferation, mitotic spindle formation, transcription factor, and oncogenesis, and up-regulates genes related to the induction of apoptosis and cell cycle arrest in prostate cancer PC-3 and LNCaP cells (6,7).

Connexins (Cxs) are a family of transmembrane proteins that enable gap junctional intercellular communication (GJIC) (8). GJIC is one mechanism of growth control that involves cell-cell contact (9). In general, cancer cells exhibit altered Cxs expression, with a profile that is often significantly reduced or undetectable. Connexin 43 (Cx43) and connexin 32 (Cx32) expressions were reduced in prostate tumor biopsy in contrast to normal prostate epithelial cells (10-13). Since Cx43 is a tumor-suppressor gene, Cx43 gene therapy was reported (14-16). Transfection of Cx43 in human mammary carcinoma MDA-MB-435 cells (17), human glioblastoma U251 and T98G cells (16), lung cancer PG cells (18) and prostate cancer LNCaP cells (19) significantly reduces cell growth *in vitro* and/or *in vivo*. Transfection of Cx43 in human glioblastoma U251 cells (20) and ovarian carcinoma SKOV-3 cells (21) increased sensitivity to several chemotherapeutic agents. However, the effect of transfection of the Cx gene combined with DTX on prostate tumor PC-3 cells has not been reported to our knowledge.

In this study, we investigated whether the transfection of plasmid DNA (pCMV-Cx43) coding for the Cx43 gene by non-viral vector combined with DTX increased the inhibition of PC-3 cell growth. A novel combination of pCMV-Cx43 and DTX induced significantly greater growth inhibition in PC-3 cells and tumor xenografts than DTX alone. This combination increased apoptosis via the down-regulation of Bcl-2 expression and up-regulation of caspase-3 activity.

Materials and methods

Cell culture. PC-3 and LNCaP cells were supplied by the Cell Resource Center for Biomedical Research, Tohoku University.

Correspondence to: Professor Yoshie Maitani, Institute of Medicinal Chemistry, Hoshi University, Shinagawa-ku, Tokyo 142-8501, Japan
E-mail: yoshie@hoshi.ac.jp

Key words: prostate cancer, connexin 43, docetaxel, PC-3 cells, cytotoxicity, gene therapy, non-viral vector, combination therapy

PC-3 and LNCaP cells were grown in RPMI-1640 medium supplemented with 10% heat-inactivated fetal bovine serum (FBS) and kanamycin (100 μg/ml) at 37°C in a 5% CO_2 humidified atmosphere.

Plasmid constructions. Plasmid pCMV-Cx43 encoding the Cx43 gene under the control of CMV promoter was constructed as previously described (22). Plasmid pCMV-luc encoding the luciferase gene under the control of the CMV promoter was constructed as previously described (23). pGL3-basic (Promega, Madison, WI) was used as a control plasmid. A protein-free preparation of the plasmid was purified following alkaline lysis using maxiprep columns (Qiagen, Hilden, Germany).

Sensitivity to DTX assay. PC-3 and LNCaP cells were seeded separately at a density of $1x10^4$ cells per well in 96-well plates and maintained for 24 h before transfection in RPMI medium supplemented with 10% FBS. Cells at 30% confluence in the well were transfected with 0.2 μg of pCMV-Cx43 or pGL3-basic using lipofectamine 2000 (Invitrogen Corp., Carlsbad, CA) according to the manufacturer's instructions and incubated for 24 h. The culture medium was then exchanged to medium containing various concentrations of DTX (Taxotere, Sanofi-Aventis, Paris, France) ranging from 0.1 to 1,000 ng/ml and incubated for another 48 h. In co-transfection, cells were transfected with 0.2 μg of pCMV-Cx43 or pGL3-basic using lipofectamine 2000 in medium containing DTX (0.1-1,000 ng/ml) and incubated for 72 h. The cell number was determined with WST-8 assay (Dojindo Laboratories, Kumamoto, Japan).

Fluorescent dye transfer. FACS analysis of the GJIC reported by Robe *et al* (24) was modified. Briefly, cells grown in 35-mm dishes were labeled for 1-h incubation with either 5 μM calcein-AM (acetomethylic ester, Dojindo) or 5 μM DiI (Lambda Probes & Diagnostics, Graz, Austria) in the medium. The two labeled cells were mixed in equal proportions in 35-mm dishes and incubated for 12 h. Subsequently, pCMV-Cx43 or pGL3-basic was transfected into mixed cells in the presence or absence of 50 μM 18α-glycyrrhethinic acid (18GA, MP Biomedicals, Germany). After 24-h incubation, the cells were trypsinized, washed in phosphate-buffered saline pH 7.4 (PBS), and processed for FACS analysis of calcein-AM and DiI fluorescence with a FACSCalibur flow cytometer as previously reported (22). Data for 10,000 fluorescent events were obtained by calcein-AM fluorescence (530/30 nm) and DiI fluorescence (585/42).

Cell cycle analysis. PC-3 cells were seeded at a density of $1x10^6$ cells on 35-mm dishes. Cells were transfected with pCMV-Cx43 or pGL3-basic in the presence or absence of 10 ng/ml DTX in medium. After 24-h incubation, the cells were harvested with EDTA after washing with ice-cold PBS. Detached cells were washed once with ice-cold PBS and gently suspended in PBS-EtOH (70%) and fixed overnight at 4°C. For staining, fixed cells were washed once in PBS and then resuspended in PBS with 50 μg/ml propidium iodide (PI) and 0.5% RNase A. After 30 min at 37°C, cells were processed for FACS analysis of PI fluorescence by a FACSCalibur flow cytometer as described in the above section.

Western blotting. PC-3 cells were seeded at a density of $1x10^6$ cells on 35-mm dishes. Cells were transfected with pGL3-basic or pCMV-Cx43, respectively. Twenty-four hours after transfection, the culture medium was replaced with medium containing 10 ng/ml DTX and incubated for 24 h. Cells were suspended in lysis buffer (1% Triton-X 100 and protease inhibitor cocktail set III (Calbiochem, Darmstadt, Germany) in PBS), and then centrifuged at 15,000 rpm for 10 min. The supernatants were resolved on a 15% sodium dodecyl sulphate-polyacrylamide gel by electrophoresis (SDS-PAGE) and transferred to a polyvinylidene difluoride (PVDF) membrane (FluoroTrans® W, PALL Gelman Laboratory, Ann Arbor, MI). Expression of Cx43, Bcl-2 and ß-actin protein was identified using rabbit anti-Cx43 polyclonal antibody (Sigma, St. Louis, MO), rabbit anti-Bcl-2 polyclonal antibody (Stressgen, Canada) or rabbit anti-ß-actin polyclonal antibody (Lab Vision, CA), respectively. Goat anti-rabbit IgG peroxidase conjugate (Santa Cruz Biotechnology, Inc., Santa Cruz, CA) was used as the secondary antibody. These proteins were detected with peroxidase-induced chemiluminescence (Super Signal West Pico Chemiluminescent Substrate, Pierce). Optical density of the bands on the film was quantified using ImageQuant TL (Amersham Biosciences, NJ) with correction for the optical density of the corresponding ß-actin band.

Apoptosis analysis. PC-3 cells were seeded at a density of $1x10^6$ cells on 35-mm dishes. The cells were transfected with pGL3-basic or pCMV-Cx43, respectively. Twenty-four hours after transfection, the culture medium was replaced with medium containing 10 ng/ml DTX and incubated for 24 h. Apoptotic cells were detected with an annexin V-FITC apoptosis detection kit (Sigma) or caspase-3 apoptosis detection kit (Santa Cruz Biotechnology) according to the manufacturer's instructions.

Assessment of PC-3 tumor growth. For transfection *in vivo*, we prepared cationic nanoparticle (NP) as previously reported (25). Briefly, NP was formulated using 1 mg/ml cholesteryl-3ß-carboxyamidoethylene-*N*-hydroxyethylamine (OH-Chol) as a cationic lipid, and 5 mol% Tween-80, and was prepared in 10 ml of water by the modified ethanol injection method (25).

Male BALB/c nu/nu mice (6-8 weeks of age) were purchased from CLEA Japan Inc. (Tokyo, Japan). To generate PC-3 tumor xenografts, $1x10^7$ PC-3 cells suspended in 50 ml of medium containing 60% reconstituted basement membrane (Matrigel: Collaborative Research, Bedford, MA) were inoculated subcutaneously into the flank region of the mice. Tumor volume was calculated using the formula, tumor volume = $0.5ab^2$, where a and b are the larger and smaller diameters, respectively. When the average volume of PC-3 xenograft tumors reached 200 mm^3 (day 0), these mice were selected for treatment with DTX alone, pGL3-basic, pCMV-Cx43, pGL3-basic plus DTX, and pCMV-Cx43 plus DTX. For transfection into tumors, the nanoplex was formed by the addition of NP (15.8 μl) to 10 μg of pCMV-Cx43 or pGL3-basic with gentle shaking and standing at room temperature for 10 min. Nanoplexes of 10 μg plasmid per tumor were directly injected into xenografts on days 0 and 1. DTX at a dose of 15 mg/kg was injected i.v. on day 0. Tumor volume was measured on days 0, 3, 6, 9, 11, 13, 15. On day 15, all

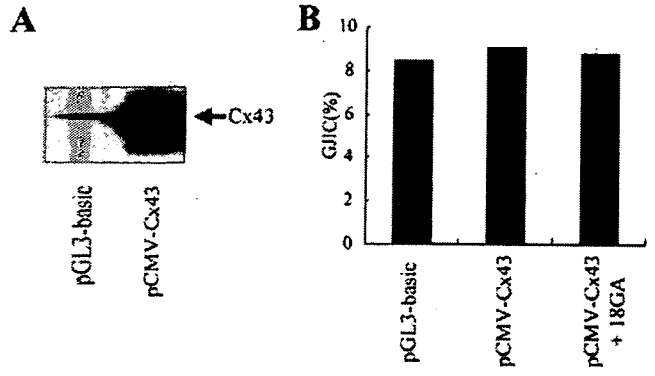

Figure 1. Cx43 expression and GJIC transfected with pCMV-Cx43 in PC-3 cells. (A) Western blot analyses of Cx43 in the cells 24 h after transfection with pCMV-Cx43 or pGL3-basic. (B) Effect of Cx43 transfection on gap junctional intercellular communication (GJIC) analyzed by flow cytometry. Calcein-AM-labeled cells were mixed with DiI-labeled cells, and transfected with pCMV-Cx43 or pGL3-basic. Cells were incubated for 24 h in the presence or absence of 50 μM 18GA.

mice were sacrificed after anesthetization by i.m. injection of pentobarbital (Nembutal, Dainippon Pharmaceutical Co., Ltd., Osaka, Japan), and the tumor weights were measured. The data are shown as the mean ± SE. Animal experiments were conducted with ethical approval from our institutional animal care and use committee.

Statistical analysis. The statistical significance of the data was evaluated with Student's t-test. A $P \leq 0.05$ was considered significant.

Results

Effect of Cx43 expression on PC-3 cells. We initially characterized the expression of Cx43 in PC-3 cells. In this study, we used pGL3-basic as a control plasmid. Cx43 expression was observed strongly in pCMV-Cx43-transfected cells, but weakly in pGL3-basic-transfected cells (Fig. 1A). Next, we examined whether the transfection of pCMV-Cx43 induced growth inhibition in the cells. Seventy-two hours after transfection, Cx43 expression did not significantly induce a suppressive effect in PC-3 cells (data not shown).

To investigate whether the expression of Cx43 protein by pCMV-Cx43 caused the formation of gap junctions, we assessed the transfer of calcein-AM, a cytoplasmic dye that crosses gap junctions, in co-culture with calcein-AM-loaded cells and cells marked with DiI, a non-diffusible membrane fluorescent dye, by FACS analysis. As shown in Fig. 1B, GJIC (%) was not significantly increased in pCMV-Cx43-transfected cells compared with pGL3-basic-transfected cells. Moreover, pCMV-Cx43-transfected cells treated with 18GA, GJIC inhibitor did not decrease either the GJIC (%) compared with pGL3-basic- or pCMV-Cx43-transfected cells (Fig. 1B).

In vitro sensitivity of DTX. To evaluate the *in vitro* growth inhibitory effect of combination therapy of Cx43 and DTX, the WST-8 assay was initially performed. When PC-3 cells were transfected with pGL3-basic or pCMV-Cx43 in the presence of DTX, pCMV-Cx43-transfected cells (IC_{50} = 1.1 ng/ml) showed 53-fold higher sensitivity to DTX than pGL3-basic-transfected cells (IC_{50} = 58.7 ng/ml) (Fig. 2A). However, when PC-3 cells were treated with DTX 24 h after the transfection of pGL3-basic or pCMV-Cx43, pCMV-Cx43-transfected cells (IC_{50} = 1.4 ng/ml) showed 279-fold higher sensitivity to DTX than pGL3-basic-transfected cells (IC_{50} = 390.0 ng/ml) (Fig. 2B). When PC-3 cells were transfected with pCMV-Cx43 24 h after treatment with DTX, cytotoxicity could not be evaluated since cells were almost dead even at 1 ng/ml of DTX (data not shown). Therefore, in subsequent *in vitro* experiments, the cells were treated with DTX 24 h after transfection of pCMV-Cx43.

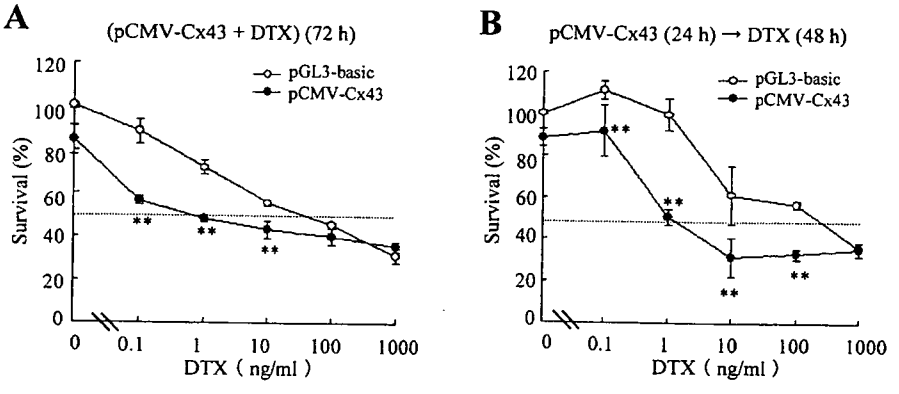

	IC_{50} (ng/ml)	(%)
pGL3-basic	58.7	100.0
pCMV-Cx43	1.1	1.8

	IC_{50} (ng/ml)	(%)
pGL3-basic	390.0	100.0
pCMV-Cx43	1.4	0.4

Figure 2. Concentration-dependent effect of DTX on cytotoxicity in Cx43-transfected cells. (A) Cells were transfected with 0.2 μg of pCMV-Cx43 or pGL3-basic in the presence of DTX and incubated for 72 h. (B) PC-3 cells were transfected with pCMV-Cx43 or pGL3-basic for 24 h. After incubation, cells were treated with various concentrations of DTX and incubated for another 48 h. The number of viable cells was determined by WST-8 assay. n=3 for each sample. **p<0.01; compared with pGL3-basic.

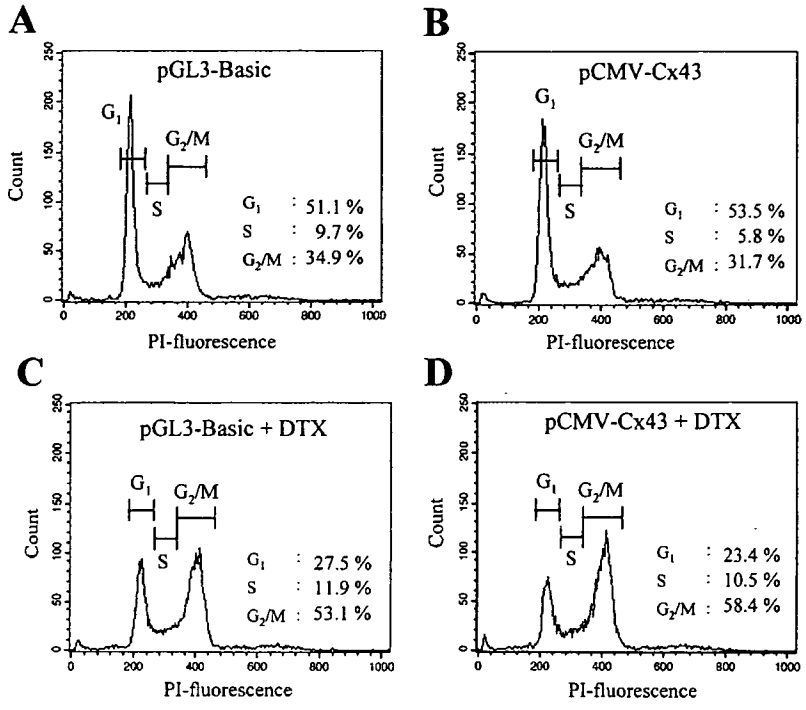

Figure 3. Cell cycle kinetics of pGL3-basic (A), pCMV-Cx43 (B), pGL3-basic plus 10 ng/ml DTX (C), and pCMV-Cx43 plus 10 ng/ml DTX (D) 24 h after transfection into PC-3 cells. Histograms illustrate the differences in G_1, S, and G_2/M phases upon transfection into PC-3 cells.

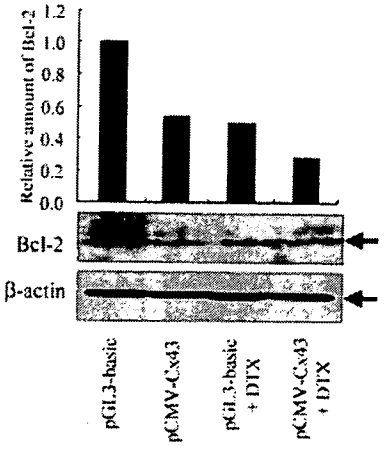

Figure 4. Decrease of Bcl-2 expression in PC-3 cells by combination therapy of Cx43 and DTX. Cells were transfected with pGL3-basic or pCMV-Cx43 for 24 h. Culture medium was replaced with medium containing of 10 ng/ml DTX and incubated for another 24 h. Bcl-2 expression was examined by Western blot analyses, quantified using densitometry.

We next assessed the effect of pCMV-Cx43 and DTX on the cell cycle 24 h after transfection into PC-3 cells by flow cytometric analysis. Transfection of pCMV-Cx43 into the cells did not affect the cell cycle (Fig. 3A and B), but DTX caused an increase in G_2/M populations (53.1%) (Fig. 3C). Co-transfection of pCMV-Cx43 with DTX resulted in substantial accumulation in G_2 (58.4%) populations (Fig. 3D).

Effect of Bcl-2 expression and apoptosis activity on PC-3 cells. Recently, it has been reported that transfection of Cx down-regulated the levels of Bcl-2 (20,26,27). Therefore, to investigate whether transfection with pCMV-Cx43 and/or treatment with DTX affected Bcl-2 expression in PC-3 cells, we examined the levels of protein expression of Bcl-2 in the cells by Western blotting. Either pCMV-Cx43-transfection or DTX treatment down-regulated the levels of Bcl-2 (Fig. 4). Moreover, pCMV-Cx43-transfected cells treated with DTX exhibited the most down-regulated level of Bcl-2 compared with pGL3-basic-transfected cells (Fig. 4).

Next, we examined the apoptotic effect in cells transfected with Cx43 and/or treated with DTX by annexin V assay. As shown in Fig. 5A, pCMV-Cx43 transfection or treatment with DTX increased apoptosis in the cells compared with pGL3-basic transfection. Moreover, the incidence of apoptosis was highest in pCMV-Cx43-transfected cells treated with DTX.

To investigate the apoptosis mechanism by combination therapy of Cx43 and DTX, we measured caspase-3 activity. As shown in Fig. 5B, caspase-3 activity in pCMV-Cx43-transfected cells, pGL3-basic-transfected cells with DTX and pCMV-Cx43-transfected cells with DTX was 1.6-, 1.4- and 2.0-fold higher than that in pGL3-basic-transfected cells, respectively. Forced expression of Cx43 in the cells induced significantly more up-regulation of caspase-3 activity than either treatment alone. These results suggest that the constitutive expression of Cx43 may play a role in the enhancement of apoptosis by chemotherapeutic agents.

Synergistic inhibition of the growth of PC-3 tumor xenografts. The efficacy of combination therapy of Cx43 and DTX in inhibiting the growth of subcutaneous PC-3 tumors was evaluated. We previously reported that NP could efficiently

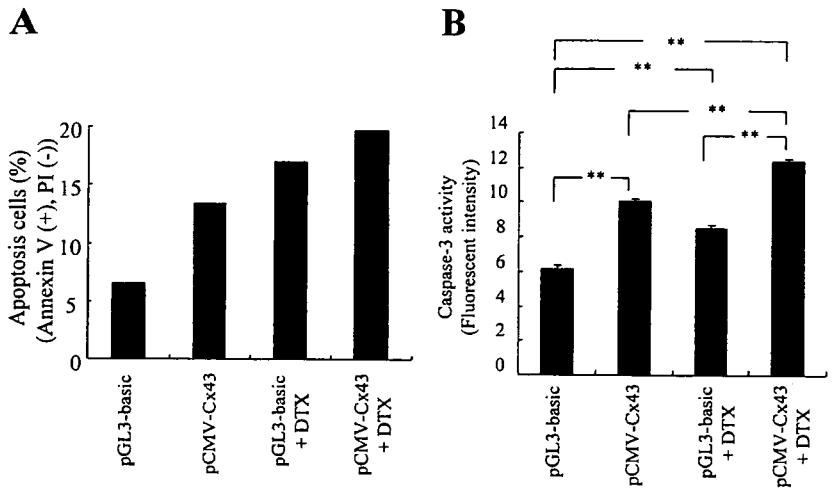

Figure 5. Apoptotic cells and caspase-3 activity by combined treatment with Cx43 and DTX on PC-3 cells. Cells were transfected with pGL3-basic or pCMV-Cx43 and incubated for 24 h. Culture medium was replaced with medium containing 10 ng/ml DTX, and incubated for another 24 h. Apoptotic cells and caspase-3 activity were detected by annexin V assay (A) and caspase-3 fluorometric assay (B). (B), n=3 for each sample. **p<0.01.

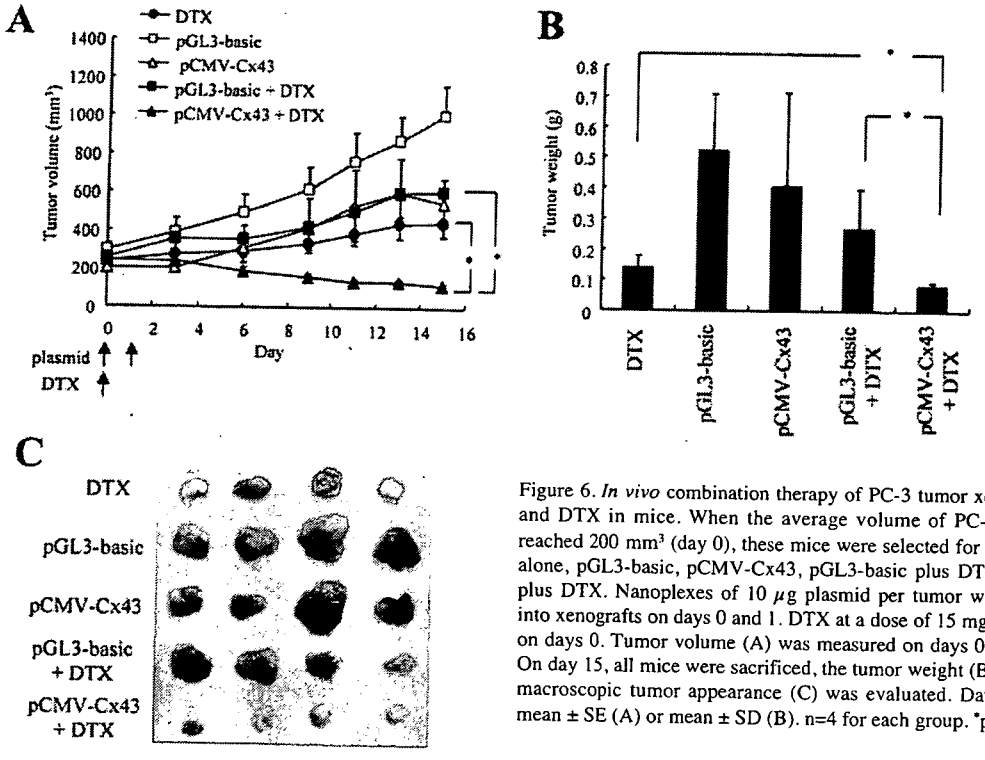

Figure 6. *In vivo* combination therapy of PC-3 tumor xenografts with Cx43 and DTX in mice. When the average volume of PC-3 xenograft tumors reached 200 mm³ (day 0), these mice were selected for treatment with DTX alone, pGL3-basic, pCMV-Cx43, pGL3-basic plus DTX and pCMV-Cx43 plus DTX. Nanoplexes of 10 μg plasmid per tumor were directly injected into xenografts on days 0 and 1. DTX at a dose of 15 mg/kg was injected i.v. on days 0. Tumor volume (A) was measured on days 0, 3, 6, 9, 11, 13, 15. On day 15, all mice were sacrificed, the tumor weight (B) was measured and macroscopic tumor appearance (C) was evaluated. Data are shown as the mean ± SE (A) or mean ± SD (B). n=4 for each group. *p<0.05.

deliver DNA into PC-3 xenografts (28). Therefore, we used NP as a DNA transfection vector for *in vivo* experiment. The anti-tumor effect was evaluated by direct injection of the nanoplex of pCMV-Cx43 or pGL3-basic into the xenografts once a day on two occasions (day 0 and 1) following one i.v. injection of DTX (day 0) according to a previous report on *in vivo* combination gene therapy with DTX (29). No significant decrease in tumor weight was observed in mice treated with pCMV-Cx43 (Fig. 6B). A growth inhibitory effect was observed in mice treated with DTX alone or pGL3-basic plus DTX compared with control mice (Fig. 6A and B). pGL3-basic plus DTX exhibited a similar tumor suppressive effect with DTX alone, indicating that DNA transfection did not increase tumor growth inhibition. A significant growth inhibitory effect was observed in combination therapy of pCMV-Cx43 and DTX compared with DTX alone (Fig. 6A and B). A comparison of tumor weight and the appearance after excision also demonstrated that tumor growth was attenuated in mice treated with pCMV-Cx43 and DTX (Fig. 6B and C).

Discussion

The limited efficacy of cytotoxic chemotherapy remains a major problem in the treatment of advanced hormone-refractory prostate cancer (30); therefore, novel cancer gene therapy needs to be developed. In this study, we found that Cx43 expression in PC-3 cells significantly enhanced DTX cytotoxicity through down-regulation of Bcl-2 expression and activation of the apoptosis pathway. Furthermore, the combination of non-viral Cx43 gene therapy and DTX significantly suppressed the growth of tumor xenografts compared to DTX alone. This is the first report to highlight that the expression of Cx43 in association with DTX has potential as a tumor growth inhibitor.

Dysregulation of Cx expression is thought to be associated with carcinogenesis; however, there is relatively little information regarding the mechanism of altered Cx expression in prostate cancer. The tumor-suppressing effects of Cx genes largely depend on the Cx species and the cell types used (31). Transduction of Cx32 and Cx43 by retroviral gene transfection into the Cx-deficient prostate cancer cell line LNCaP produced growth inhibition *in vitro* and *in vivo*, and cell differentiation associated with gap junction formation (19). Transduction of Cx26 by adenoviral gene transfection into LNCaP and PC-3 cells produced growth inhibition by a GJIC function (26). Regarding Cx43, the expression of Cx43 in PC-3 cells could not form gap junctions (32). In our study, the transfection of pCMV-Cx43 into PC-3 cells exhibited neither the inhibition of cell growth nor increased GJIC (Fig. 1); however, transfection into the cells increased apoptotic cells and caspase-3 activity (Fig. 5). Cx43 expression in PC-3 cells might regulate apoptosis via a GJIC-independent mechanism.

Combination therapy of Cx43 and DTX was significantly more cytotoxic when cells were treated with DTX 24 h after Cx43 transfection compared with treatment with DTX and transfection at the same time. It suggested that Cx43 expression 24 h after transfection affected sensitivity to DTX. We also found that combination therapy 72 h after transfection increased growth inhibition in LNCaP cells (IC_{50} for DTX = 32 and 4.2 ng/ml in pGL3-basic- and pCMV-Cx43-transfected cells, respectively) (data not shown). Combination therapy using the Cx gene and chemotherapeutic agents for cancer has been reported. Cx43 transfected into human glioblastoma cells (20) and ovarian carcinoma cells (21) led to the down-regulation of Bcl-2 and increased sensitivity to paclitaxel and doxorubicin. In our study, DTX treatment caused an increase in G_2/M populations into PC-3 cells (Fig. 3C), and also induced the down-regulation of Bcl-2 expression and up-regulation of caspase-3 activity in PC-3 cells (Figs. 4 and 5). This finding corresponds with previous reports that DTX induced the down-regulation of Bcl-2 expression in prostate tumor LNCaP and PC-3 cells (33,34), and that down-regulation of Bcl-2 expression by Bcl-2 antisense activated caspase-3 activity in PC-3 cells (35). Combination therapy of pCMV-Cx43 and DTX increased G_2/M populations, enhancing down-regulation of Bcl-2, and growth inhibition *in vitro* more than DTX alone.

The combination of repeated intratumoral injections of pCMV-Cx43 (10 μg/tumor) with non-viral vector and a single intravenous injection of DTX (15 mg/kg) was compared with a repeated injection of Cx43 alone and a single injection of DTX alone in PC-3 tumor xenografts. Significant antitumoral effects were observed in mice receiving combined treatment, compared with DTX alone. The efficacy *in vivo* might result from direct effects of Cx43 on inducing apoptosis and indirect effects on enhancing the cytotoxicity of DTX by down-regulating Bcl-2. It has been reported that paclitaxel increased the transfection efficiency of cationic liposome by inhibiting targeting endosomes to lysosomes (36,37). Therefore, using the combined lipid-mediated transfection of genes with DTX for cancer gene therapy might be a powerful technique due to the effect of enhanced gene expression. Inhibiting Bcl-2 expression by Cx43 in prostate cancer cells, which could restore their sensitivity to chemotherapeutic agents, would be a new therapeutic strategy against prostate cancer.

From a clinical point of view, the doses of DTX used in the combined strategy will be minimal, and will prevent significant toxicity due to DTX. Low doses of DTX can thus be administered in humans for a prolonged period of time, or alternatively, a shorter duration of combined treatment may be administered without loss of effectiveness. Enforced expression of Cx43 increased sensitivity for DTX via the down-regulation of Bcl-2 expression in PC-3 cells. Combining non-viral Cx43 gene therapy with DTX resulted in greater growth suppression of PC-3 *in vitro* and *in vivo*. The data presented here provide a rational strategy for treating patients with advanced hormone refractory prostate cancer.

Acknowledgements

This project was supported in part by a grant from The Promotion and Mutual Aid Corporation for Private Schools of Japan, and by a Grant-in-aid for Scientific Research from the Ministry of Education, Culture, Sports, Science, and Technology of Japan.

References

1. Gao X, Porter AT, Grignon DJ, Pontes JE and Honn KV: Diagnostic and prognostic markers for human prostate cancer. Prostate 31: 264-281, 1997.
2. Oh WK and Kantoff PW: Management of hormone refractory prostate cancer: current standards and future prospects. J Urol 160: 1220-1229, 1998.
3. Syed S: Combination chemotherapy for hormone-refractory prostate carcinoma: progress and pitfalls. Cancer 98: 2088-2090, 2003.
4. Beer TM, El Geneidi M and Eilers KM: Docetaxel (taxotere) in the treatment of prostate cancer. Expert Rev Anticancer Ther 3: 261-268, 2003.
5. Hong WK: The current status of docetaxel in solid tumors. An M.D. Anderson Cancer Center Review. Oncology 16: 9-15, 2002.
6. Pienta KJ: Preclinical mechanisms of action of docetaxel and docetaxel combinations in prostate cancer. Semin Oncol 28: 3-7, 2001.
7. Li Y, Li X, Hussain M and Sarkar FH: Regulation of microtubule, apoptosis, and cell cycle-related genes by taxotere in prostate cancer cells analyzed by microarray. Neoplasia 6: 158-167, 2004.
8. Knuechel R, Siebert-Wellnhofer A, Traub O and Dermietzel R: Connexin expression and intercellular communication in two- and three-dimensional *in vitro* cultures of human bladder carcinoma. Am J Pathol 149: 1321-1332, 1996.
9. Bruzzone R, White TW and Paul DL: Connections with connexins: the molecular basis of direct intercellular signaling. Eur J Biochem 238: 1-27, 1996.

10. Tsai H, Werber J, Davia MO, *et al*: Reduced connexin 43 expression in high grade, human prostatic adenocarcinoma cells. Biochem Biophys Res Commun 227: 64-69, 1996.
11. Hossain MZ, Jagdale AB, Ao P, LeCiel C, Huang RP and Boynton AL: Impaired expression and posttranslational processing of connexin43 and downregulation of gap junctional communication in neoplastic human prostate cells. Prostate 38: 55-59, 1999.
12. Habermann H, Ray V, Habermann W and Prins GS: Alterations in gap junction protein expression in human benign prostatic hyperplasia and prostate cancer. J Urol 167: 655-660, 2002.
13. Mehta PP, Lokeshwar BL, Schiller PC, Bendix MV, Ostenson RC, Howard GA and Roos BA: Gap-junctional communication in normal and neoplastic prostate epithelial cells and its regulation by cAMP. Mol Carcinog 15: 18-32, 1996.
14. Yamasaki H: Role of disrupted gap junctional intercellular communication in detection and characterization of carcinogens. Mutat Res 365: 91-105, 1996.
15. Chen SC, Pelletier DB, Ao P and Boynton AL: Connexin43 reverses the phenotype of transformed cells and alters their expression of cyclin/cyclin-dependent kinases. Cell Growth Differ 6: 681-690, 1995.
16. Huang RP, Fan Y, Hossain MZ, Peng A, Zeng ZL and Boynton AL: Reversion of the neoplastic phenotype of human glioblastoma cells by connexin 43 (cx43). Cancer Res 58: 5089-5096, 1998.
17. Hirschi KK, Xu CE, Tsukamoto T and Sager R: Gap junction genes Cx26 and Cx43 individually suppress the cancer phenotype of human mammary carcinoma cells and restore differentiation potential. Cell Growth Differ 7: 861-870, 1996.
18. Zhang ZQ, Zhang W, Wang NQ, Bani-Yaghoub M, Lin ZX and Naus CC: Suppression of tumorigenicity of human lung carcinoma cells after transfection with connexin43. Carcinogenesis 19: 1889-1894, 1998.
19. Mehta PP, Perez-Stable C, Nadji M, Mian M, Asotra K and Roos BA: Suppression of human prostate cancer cell growth by forced expression of connexin genes. Dev Genet 24: 91-110, 1999.
20. Huang RP, Hossain MZ, Huang R, Gano J, Fan Y and Boynton AL: Connexin 43 (cx43) enhances chemotherapy-induced apoptosis in human glioblastoma cells. Int J Cancer 92: 130-138, 2001.
21. Fernstrom MJ, Koffler LD, Abou-Rjaily G, Boucher PD, Shewach DS and Ruch RJ: Neoplastic reversal of human ovarian carcinoma cells transfected with connexin 43. Exp Mol Pathol 73: 54-60, 2002.
22. Hattori Y and Maitani Y: Folate-linked nanoparticle-mediated suicide gene therapy in human prostate cancer and nasopharyngeal cancer with herpes simplex virus thymidine kinase. Cancer Gene Ther 12: 796-809, 2005.
23. Igarashi S, Hattori Y and Maitani Y: Biosurfactant MEL-A enhances cellular association and gene transfection by cationic liposome. J Control Release 112: 362-368, 2006.
24. Robe PA, Jolois O, N'Guyen M, Princen F, Malgrange B, Merville MP and Bours V: Modulation of the HSV-TK/ganciclovir bystander effect by n-butyrate in glioblastoma: correlation with gap-junction intercellular communication. Int J Oncol 25: 187-192, 2004.
25. Hattori Y, Kubo H, Higashiyama K and Maitani Y: Folate-linked nanoparticles formed with DNA complexes in sodium chloride solution enhance transfection efficiency. J Biomed Nanotech 1: 176-184, 2005.
26. Tanaka M and Grossman HB: Connexin 26 induces growth suppression, apoptosis and increased efficacy of doxorubicin in prostate cancer cells. Oncol Rep 11: 537-541, 2004.
27. Fujimoto E, Sato H, Nagashima Y, *et al*: A Src family inhibitor (PP1) potentiates tumor-suppressive effect of connexin 32 gene in renal cancer cells. Life Sci 76: 2711-2720, 2005.
28. Hattori Y and Maitani Y: Two-step transcriptional amplification-lipid-based nanoparticles using PSMA or midkine promoter for suicide gene therapy in prostate cancer. Cancer Sci 97: 787-798, 2006.
29. Hayashi N, Asano K, Suzuki H, Yamamoto T, Tanigawa N, Egawa S and Manome Y: Adenoviral infection of survivin antisense sensitizes prostate cancer cells to etoposide *in vivo*. Prostate 65: 10-19, 2005.
30. Kasamon KM and Dawson NA: Update on hormone-refractory prostate cancer. Curr Opin Urol 14: 185-193, 2004.
31. Mesnil M, Krutovskikh V, Piccoli C, Elfgang C, Traub O, Willecke K and Yamasaki H: Negative growth control of HeLa cells by connexin genes: connexin species specificity. Cancer Res 55: 629-639, 1995.
32. Govindarajan R, Zhao S, Song XH, Guo RJ, Wheelock M, Johnson KR and Mehta PP: Impaired trafficking of connexins in androgen-independent human prostate cancer cell lines and its mitigation by alpha-catenin. J Biol Chem 277: 50087-50097, 2002.
33. Tang Y, Khan MA, Goloubeva O, Lee DI, Jelovac D, Brodie AM and Hussain A: Docetaxel followed by castration improves outcomes in LNCaP prostate cancer-bearing severe combined immunodeficient mice. Clin Cancer Res 12: 169-174, 2006.
34. Muramaki M, Miyake H, Hara I and Kamidono S: Synergistic inhibition of tumor growth and metastasis by combined treatment with TNP-470 and docetaxel in a human prostate cancer PC-3 model. Int J Oncol 26: 623-628, 2005.
35. Yamanaka K, Rocchi P, Miyake H, Fazli L, Vessella B, Zangemeister-Wittke U and Gleave ME: A novel antisense oligonucleotide inhibiting several antiapoptotic Bcl-2 family members induces apoptosis and enhances chemosensitivity in androgen-independent human prostate cancer PC3 cells. Mol Cancer Ther 4: 1689-1698, 2005.
36. Hasegawa S, Hirashima N and Nakanishi M: Microtubule involvement in the intracellular dynamics for gene transfection mediated by cationic liposomes. Gene Ther 8: 1669-1673, 2001.
37. Nair RR, Rodgers JR and Schwarz LA: Enhancement of transgene expression by combining glucocorticoids and anti-mitotic agents during transient transfection using DNA-cationic liposomes. Mol Ther 5: 455-462, 2002.